



## Oxidized multiwalled carbon nanotubes for the removal of methyl red (MR): kinetics and equilibrium study

Mehrorang Ghaedi<sup>a,\*</sup>, Syamak Nasiri Kokhdan<sup>b</sup>

<sup>a</sup>Chemistry Department, Yasouj University, Yasouj 75918-74831, Iran  
Tel./Fax: +98 741 2223048; email: m\_ghaedi@mail.yu.ac.ir

<sup>b</sup>Young Researchers club, Yasooj Branch, Islamic Azad University, Yasooj, Iran

Received 8 November 2011; Accepted 10 July 2012

### ABSTRACT

Oxidized multiwalled carbon nanotubes (MWCNT) were used for the removal of methyl red (MR) from aqueous solutions. The effects of variables, such as initial solution pH, initial dye concentration, temperature, and sorption time, on MR removal were studied and optimized. Fitting the experimental equilibrium data to various investigated isotherm models, such as Langmuir, Freundlich, Tempkin, and Dubinin–Radushkevich (D–R) models, showed the suitability of the Langmuir model with the highest correlation coefficients. The calculated thermodynamic parameters indicated that the removal of MR by MWCNT is an entropy-driven and endothermic process. The experimental data were analyzed by different kinetic models, such as pseudo-first order, pseudo-second order, and Elovich and intraparticle diffusion models. It was found that the second-order equation and intraparticle diffusion models are the rate-limiting factor and control the kinetic of the adsorption process.

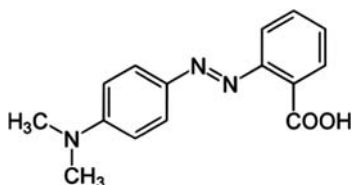
*Keywords:* Adsorption; Methyl red (MR); Multiwalled carbon nanotube; Kinetics and thermodynamics of adsorption

### 1. Introduction

Because of the large amount of wastewater produced by the textile industries, the removal of dyes from these industrial effluents is an important application to produce a safe and clean environment [1]. Azo dyes, one of the synthetic applied dyes in many textiles industries [2] with azo group ( $-N=N-$ ), are low cost, soluble, and stable. Azo dyes and their intermediate products are toxic, carcinogenic, and mutagenic to aquatic life [3–5]. Some of the applied techniques for the treatment of dyes contaminated wastewaters are flocculation, coagulation, precipitation, adsorption, membrane filtration, electrochemical techniques, ozonation, and fungal decolorization [6]. Among them the adsorption based procedure is widely utilized due to

its high efficiency, capacity, and ability for large scale dye removal application (with potential for adsorbent regeneration) [7–17]. The nontoxic, low cost, and easy available adsorbents are the best choice for wastewater treatment. Multiwalled carbon nanotubes (MWCNTs) are one of the most commonly used building blocks of nanotechnology. MWCNTs are unique and one-dimensional macromolecules that possess outstanding thermal and chemical stability [18]. These nanomaterials have been proven to possess great potential as adsorbents for removing many kinds of environmental pollutants [19]. MWCNTs have been considered useful in pollution prevention strategies and are known to have widespread applications as environmental adsorbents and high-flux membranes [20] and are also potentially important for *in situ* environmental remediation due to their unique properties and high reactivity [21,22].

\*Corresponding author.



Scheme 1. Chemical structure of MR.

In this research, the MWCNT was oxidized and used as an efficient adsorbent for the removal of methyl red (MR) (Scheme 1). The equilibrium adsorption isotherms were investigated and the experimental data were analyzed by common isotherm models such as the Langmuir, Freundlich, Tempkin, and Dubinin–Radushkevich (D–R) isotherm models.

## 2. Materials and methods

### 2.1. Instruments and reagents

The stock MR (CAS number: 493-52-7, formula weight: 269.3 g/mol, and molecular formula:  $C_{15}H_{15}N_3O_2$ ) solution was prepared by dissolving appropriate amount of solid dye in double distilled water and the desired concentrations of test solutions were prepared by diluting the stock solution. The pH measurements were carried out using pH/Ion meter model-686 and the MR concentration remained in the dilute phase was determined using Jusco UV–vis spectrophotometer model V-530 at a wavelength of 508 nm and the morphology of the MWCNTs nano-needles was observed by field emission scanning electron microscopy (FE-SEM; Hitachi S-4160) under an acceleration voltage of 15 kV and FT-IR: 460 Jusco. All chemicals including NaOH, HCl, and KCl with the highest purity available were purchased from Merck (Darmstadt, Germany).

### 2.2. Measurements of dye uptake

The dye concentrations in the aqueous solution were estimated quantitatively using the linear regression equations obtained at different MR concentrations. The efficiency of MR removal was determined at different time intervals (in the range of 5–25 min) and the equilibrium was established after 25 min of contact time. The effect of initial pH on the removal of MR was evaluated in the pH range of 1–10, by contacting 20 mg/L of initial dye concentration with 0.4 g/L of oxidized-MWCNT for 25 min of contact time. The experiments were also performed in the initial MR concentration range of 5–60 mg/L to obtain adsorption isotherms.

The adsorbed MR amount ( $q_e$  mg/g) was calculated by the following mass balance relationship:

$$q_e = (C_0 - C_e)V/W \quad (1)$$

where  $C_0$  and  $C_e$  ( $\text{mg L}^{-1}$ ) are the initial and equilibrium dye concentrations in aqueous solution, respectively,  $V$  (L) is the volume of the solution, and  $W$  (g) is the mass of the adsorbent.

## 3. Results and discussion

### 3.1. Characterization of adsorbent

To enhance the efficiency of MWCNTs powder, it was washed with 10% (v/v) hydrochloric acid solution while stirring the mixture for 2 h. The filtration, washing, and other treatment processes for MWCNTs were carried out according to our previous study [11]. The oxidation of MWCNT was studied by FTIR spectroscopy investigation as a powerful and acceptable protocol. The FTIR spectrum of oxidized MWCNT shows some important characteristic vibrational frequencies at 2,500–3,400 (bw), 1,627(w), 1,155(s), 673(s), and 592(s) (Fig. 1(a)) that may be assigned probably due to the hydroxyl group, carbonyl group, and presence of stretching C–O and bending C–H of aromatic, respectively, (Fig. 1(a)). The SEM image of the MWCNT, as shown in Fig. 1(b), shows the homogeneous and small particles size MWCNT that is the suitable adsorbent with high surface area. The pH corresponding to the point of zero charge ( $\text{pH}_{\text{pzc}}$ ), for the oxidized MWCNT, was determined by the pH drift method. The proposed sorbent was soaked in HCl for 24 h in order to convert any remaining sodium salt of the acid functional groups into their acidic form. After filtration, the residual material was washed several times with distilled water till neutrality ( $\text{AgNO}_3$  negative test) and dried at 105 °C. The pH drift was measured on 0.005 M NaCl solutions (20 mL) placed in jacketed titration vessels, thermostated at 298 K. Nitrogen was bubbled through the solutions to stabilize the pH. The pH was then adjusted to successive initial values between 2 and 10 by adding HCl or NaOH and MWCNT (0.06 g) was added to the solution. The final pH was measured after 48 h.

The  $\text{pH}_{\text{pzc}}$  value of the MWCNT was found to be  $2.4 \pm 0.2$ . The surface of the MWCNT is neutral when pH of the aqueous solution is equal to  $\text{pH}_{\text{pzc}}$ . At  $\text{pH} < \text{pH}_{\text{pzc}}$ , the surface of the sorbent is positively charged, because of the adsorption of  $\text{H}_3\text{O}^+$  ions by its functional groups including hydroxyl group or donating nitrogen atom. Thus, a repulsion force occurs between the dye molecules and the sorbent surface

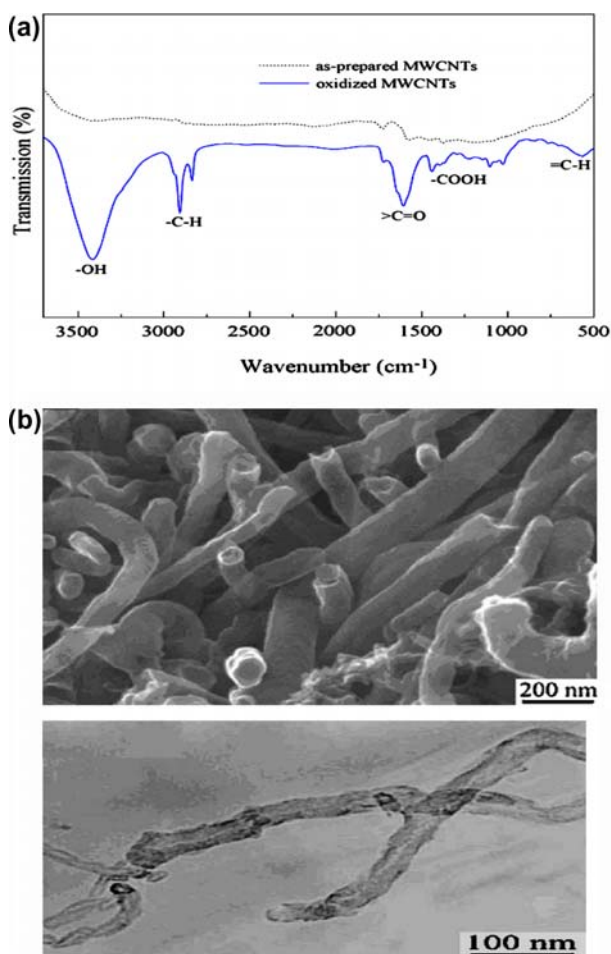


Fig. 1. (a) FT-IR spectra of oxidized MWCNTs and MWCNTs (b) SEM of oxidized MWCNTs and MWCNTs.

which causes a decrease in the adsorption percentage. The reverse situation occurs at  $\text{pH} > \text{pH}_{\text{pzc}}$ , the adsorbent surface is negatively charged due to deprotonation of its functional group that favored the dye removal.

### 3.2. Effect of initial pH

The initial pH of the aqueous solution affects both the dye aqueous chemistry and the surface binding sites of the adsorbents. The effect of initial pH on the MR removal was studied in the pH range of 1–10 with initial dye concentration of 20 mg/L and adsorbent dose of 0.4 g/L. The experiments were conducted for 25 min of contact time at room temperature and the respective results are presented in Fig. 2. As can be seen, the maximum uptake and removal of the MR was obtained at pH 4.0. The initial pH significantly affects the extent of adsorption of MR over the MWCNT and the removal percentage significantly decreased at higher pH values [12]. At initial pH

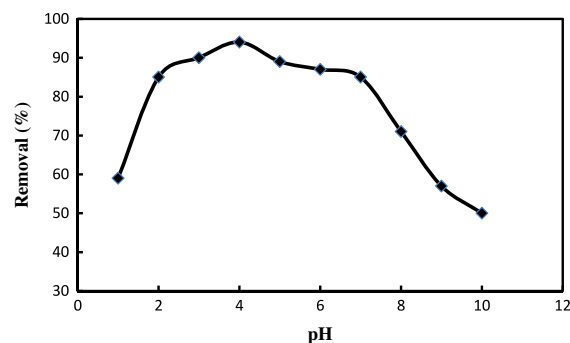


Fig. 2. Effect of pH on the removal of MR at room temperature.

lower than 4.0, as a result of protonation of the functional groups, the MWCNT surface get positively charged and the strong repulsive forces between the dye molecules and MWCNT surface lead to significant decrease in the dye removal percentage. The increase in the initial pH leads to deprotonation of the active adsorption sites on the MWCNT surface such as OH and COOH via electrostatic interaction and/or hydrogen bonding adsorb the MR molecule.

### 3.3. Effect of contact time

The equilibrium time is one of the most important parameters to design on economical wastewater treatment system. The adsorption of MR onto MWCNT was studied in various contact time to determine the adequate adsorption equilibrium time. The rapid uptake and quick establishment of equilibrium show the efficiency of particular adsorbent in terms of usage in wastewater treatment and the respective results are shown in Fig. 3. The results showed that the initial adsorption rate is rapid and gradually decrease with raising the time and reach equilibrium at about 25 min of contact time. At the initial contact time due to high diffusion of dye molecule (high its concentration gradient) into the availability of the high surface area and

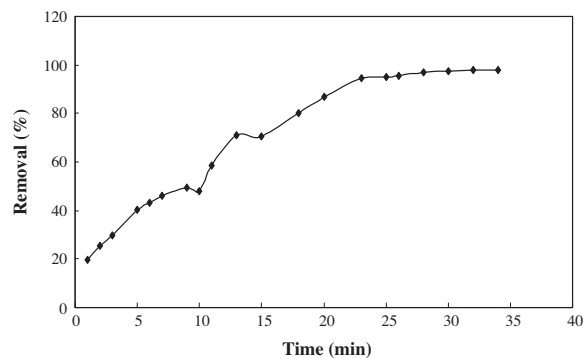


Fig. 3. Effect of contact time on removal of MR.

vacant site of MWCNT, the rate of adsorption is fast. At higher contact time due to slow rate of dye adsorption and pore diffusion of the solute into the bulk of the adsorbent, the adsorption rate significantly decreases [12]. It was found that more than 90% of MR removal was occurred in the first 20 min.

### 3.4. Effect of adsorbent dosage

One of the most critical parameter for rapid and efficient dye removal is the size and amount of adsorbents which must be optimized. The MWCNT has high tendency for adsorption of dye molecules due to its high specific surface area and small particle size. The adsorbent capacity at each dye concentration significantly depends on the amount of adsorbent. The effect of amount of MWCNTs on the MR removal percentage is shown in Fig. 4. As it is obvious, by increasing the amount of MWCNT until 0.4 g/L the MR removal percentage increased and at higher value of MWCNT the removal percentage do not change significantly. This fact can be attributed to the increase in surface area and availability of more active adsorption sites with increasing the amount of adsorbent. The dye adsorption density decreased significantly and the adsorption capacity decreased by further addition of MWCNT [11,12].

### 3.5. Effect of initial dye concentration on adsorption of MR

The effect of initial MR concentration on its removal percentage and the amount of adsorbed MR per unit mass of the adsorbent was investigated in the initial concentration range of 5–60 mg/L. It was seen that the amount of MR adsorbed per unit mass of the adsorbent increased with increasing the initial concentration, while the removal percentage decreased significantly probably due to saturation of the adsorbent surface. These phenomena emerged from the fact that initial dye concentration provides driving force to overcome the mass transfer resistance of dye between

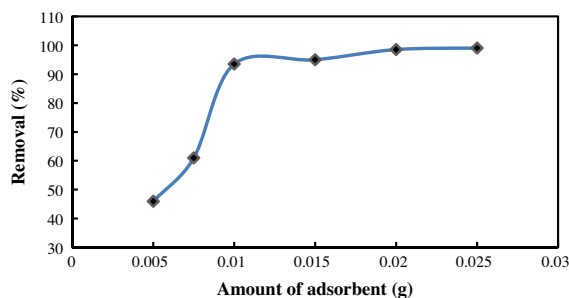


Fig. 4. Effect of adsorbent amount on MR removal at initial dye concentration of 20 mg/L.

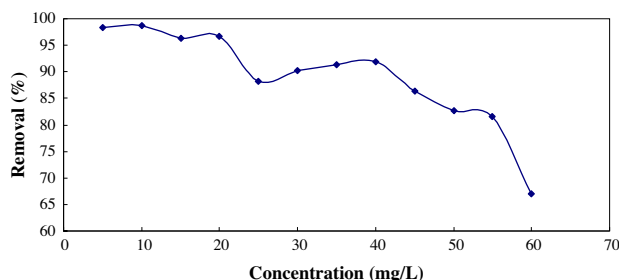


Fig. 5. Effect of initial dye concentration on MR removal at room temperature.

the aqueous and solid phases [23]. In the process, the MR molecules have to first encounter the boundary layer effect and then diffuse from the boundary layer film onto adsorbent surface and finally diffuse into the porous structure of the adsorbent that will take relatively longer contact time (Fig. 5).

### 3.6. Effect of temperature

Various textile dye effluents are produced at relatively high temperatures. Therefore, the temperature influence on the removal percentage of MR onto MWCNT was investigated as follows: a set of similar experiments were performed at different temperatures (in the range of 293–333 K) by contacting 20 mg/L of initial MR concentration at pH of 4 with 0.4 g/L of MWCNTs suspension for a contact time of 25 min. It was observed that the adsorption nature of MR onto MWCNTs depends on temperature [12].

### 3.7. Adsorption equilibrium study

The investigation of the adsorption isotherms required to attain some information about the adsorption mechanism, the surface properties, and the tendency of adsorbent toward each dye [24–28]. Several isotherm equations, such as Langmuir, Freundlich, Tempkin, and Dubinin–Radushkevich (D–R) isotherms, based on known assumption pointed out in our previous publication applied to interpret the experimental data. Based on the linear form of Langmuir isotherm model [29] (according to Table 1), the values of  $K_L$  (the Langmuir adsorption constant (L/mg)) and  $Q_m$  (theoretical maximum adsorption capacity (mg/g)) were obtained from the intercept and slope of the plot of  $C_e/q_e$  vs.  $C_e$ , respectively. The values of  $Q_m$  and  $K_L$  constants and the correlation coefficient for the Langmuir isotherm model are presented in Table 1. The high correlation coefficient shows the applicability of this model for interpretation of the experimental data over the whole concentration range.

Table 1  
Isotherm constant parameters and correlation coefficients calculated for the adsorption of MR onto MWCNT

Isotherm	Equation	Plot	Parameters	Acid red (MR)
Langmuir-1	$1/q_e = 1/(K_L Q_m C_e) + 1/Q_m$	A plot $C_e/q_e$ vs. $C_e$ should indicate a straight line of slope $1/Q_m$ and an intercept of $1/(K_L Q_m)$	$Q_m$ (mg/g) $K_L$ (L mg <sup>-1</sup> ) $R^2$	108.69 1.011 0.981
Freundlich	$\ln q_e = \ln K_F + (1/n) \ln C_e$	The values of $K_F$ and $1/n$ were determined from the intercept and slope of linear plot of $\ln q_e$ vs. $\ln C_e$ , respectively	$1/n$ $K_F$ (L/mg) $R^2$	0.3797 45.102 0.908
Tempkin	$q_e = B_1 \ln K_T + B_1 \ln C_e$	Values of $B_1$ and $K_T$ were calculated from the plot of $q_e$ against $\ln C_e$	$B_1$ $K_T \times 10^{+5}$ (L/mg) $R^2$	18.657 20.36 0.902
Dubinin and Radushkevich (D-R)	$\ln q_e = \ln Q_s - B\varepsilon^2$	The slope of the plot of $\ln q_e$ vs. $\varepsilon^2$ gives $K$ (mol <sup>2</sup> (kJ <sup>2</sup> ) <sup>-1</sup> ) and the intercept yields the adsorption capacity, $Q_m$ (mg g <sup>-1</sup> )	$Q_s$ (mg/g) $B$ $E$ (kJ/mol) = $1/(2B)^{1/2}$ $R^2$	81.288 5E-08 3.162 0.853

The parameters of Freundlich isotherm model, such as  $K_F$  ((mg/g)/(mg/L)<sup>1/n</sup>) and  $n$  (intensity of the adsorption), were calculated from the intercept and slope of the linear plot of  $\ln q_e$  vs.  $\ln C_e$ , respectively, and their values are presented in Table 1. The value of  $1/n$  for Freundlich isotherm 0.379 shows the high tendency of MR for the adsorption onto MWCNT, while lower  $R^2$  value shows its unsuitability for fitting the experimental data over the whole concentration range. The heat of the adsorption and the adsorbent–adsorbate interaction were evaluated by using Tempkin isotherm model [30]. The linearized form of the model can be given as follows:

$$q_e = B_T \ln K_T + B_T \ln C_e \quad (2)$$

$$B_T = RT/b_T \quad (3)$$

where  $B$  is the Tempkin constant related to heat of the adsorption (J mol<sup>-1</sup>),  $T$  is the absolute temperature (K),  $R$  is the universal gas constant (8.314 J/mol K), and  $K_T$  is the equilibrium binding constant (L/mg). The constants obtained for Tempkin isotherm model are given in Table 1.

Another equation used in the analysis of isotherms was proposed by Dubinin–Radushkevich (D–R). The D–R model was applied to estimate the porosity apparent free energy and the characteristic of adsorption. The D–R isotherm does not assume a homogeneous surface or constant sorption potential and its linear form can be shown in Eq. (4):

$$\ln q_e = \ln Q_m - K\varepsilon^2 \quad (4)$$

where  $K$  is a constant related to the adsorption energy,  $Q_m$  is the theoretical saturation capacity, and  $\varepsilon$  is the Polanyi potential which can be calculated from Eq. (5):

$$\varepsilon = RT \ln(1 + 1/C_e) \quad (5)$$

The slope of the plot of  $\ln q_e$  vs.  $\varepsilon^2$  gives  $K$  (mol<sup>2</sup> (kJ<sup>2</sup>)<sup>-1</sup>) and the intercept yields the  $Q_m$  (mg g<sup>-1</sup>) value.

The mean free energy of the adsorption ( $E$ ), defined as the free energy change when one mole of ion is transferred from the solution to the surface of the sorbent, can be calculated by using the following equation:

$$E = 1/\sqrt{(2K)} \quad (6)$$

The calculated D–R isotherm model constants for the adsorption of MR onto MWCNTs are given in Table 1. The value of correlation coefficient obtained from D–R model is much lower than other isotherms values mentioned above. In this case, the D–R equation represents the poorer fit of the experimental data than the other isotherm equations [11,12].

### 3.8. Kinetic study

The rate and mechanism of an adsorption process can be elucidated via kinetic study. The adsorption kinetic data were described by the Lagergren pseudo-first-order model [31].

In the first-order kinetic model, according to the equation listed in Table 2, by plotting the values of  $\log(q_e - q_t)$  vs.  $t$  may give a linear relationship that  $k_1$  and  $q_e$  values can be determined from the slope and intercept of the obtained line, respectively. If the intercept does not equal to experimental  $q_e$  value, it can be considered that the reaction is not likely to be a first-order reaction even this plot has a high correlation coefficient [32,33].

The experimental data showed a high degree of nonlinearity and poor correlation coefficient for the pseudo-first-order model. In spite of first-order model, the plot of  $t/q_t$  vs.  $t$  for the pseudo-second-order kinetic model gives a straight line with a high correlation coefficient that  $k_2$  and equilibrium adsorption capacity ( $q_e$ ) were calculated from the intercept and slope of this line, respectively. The values of  $R^2$  and closeness of experimental and theoretical adsorption capacity ( $q_e$ ) value show the applicability of the second-order model to explain and interpret the experimental data (Table 2). The  $R^2$  value for pseudo-second-order kinetic model was found to be higher (0.95) and the calculated  $q_e$  value is mainly close to the experimental adsorption capacity value [20].

The Elovich equation as another rate equation based on the adsorption capacity in linear form can be given as follows:

$$q_t = 1/\beta \ln(\alpha\beta) + 1/\beta \ln(t) \quad (7)$$

Plot of  $q_t$  vs.  $\ln(t)$  should yield a linear relationship if the Elovich is applicable with a slope of  $(1/\beta)$  and an intercept of  $(1/\beta) \ln(\alpha\beta)$ . The Elovich constants obtained from the slope and the intercept of the straight line are reported in Table 2. The correlation

coefficient higher than 0.92 shows the suitability of the model for evaluation of the adsorption process [11,12].

### 3.8.1. Intraparticle diffusion model

The dye sorption is governed by either the liquid phase mass transport rate or through the intraparticle mass transport rate. The later process possibility is explored using the intraparticle diffusion model [34,35] based on diffusive mass transfer that adsorption rate expressed in terms of the square root of time ( $t$ ) is given as follows [36]:

$$q_t = k_{id}t^{0.5} + C \quad (8)$$

The values of  $K_{diff}$  and  $C$  were calculated from the slope and intercept of the plot of  $q_t$  vs.  $t^{1/2}$ .  $C$  value related to the thickness of the boundary layer and  $K_{diff}$  value the intraparticle diffusion rate constant ( $\text{mg}/(\text{g min}^{1/2})$ ) are reported in Table 2. The values of  $q_t$  were found to give two lines part with values of  $t^{1/2}$  and the rate constant  $K_{diff}$  directly evaluated from the slope of the second regression line. The first one of these lines representing surface adsorption at the beginning of the reaction and the second one is the intraparticle diffusion at the end of the reaction [36,37]. The first line shows a boundary layer effect at the initial stage of the adsorption. The second line is the gradual adsorption stage, where intraparticle diffusion is the rate limiting step. In some cases, the last and third lines show the final equilibrium stage (to slow down of intraparticle diffusion). The values of  $k_{id}$  and  $C$  were obtained from the final linear portion and their values are presented in Table 2. Since, the intraparticle curve did not pass through the origin; one can notice that in addition to

Table 2  
Kinetic parameters for the adsorption of acid red (MR) onto MWCNT

Model	Equation	Plot	Parameters	MR
First-order kinetic	$\log(q_e - q_t) = \log(q_e) - k_1/2.303t$	Plot the values of $\log(q_e - q_t)$ vs. $t$ to give a linear relationship from which $k_1$ and $q_e$ can be determined from the slope and intercept, respectively	$k_1 \times 10^{-3}$	0.46
			$q_e$ (calc)	82.21
			$R^2$	0.772
Second-order kinetic	$(t/q_t) = 1/(k_2q_e^2) + 1/q_e(t)$	Plot the values of $(t/q_t)$ vs. $t$ to give a linear relationship from which $k_1$ and $q_e$ can be determined from the slope and intercept, respectively	$k_2 \times 10^{-4}$	0.22
			$q_e$ (calc)	66.67
			$R^2$	0.955
Intraparticle diffusion	$q_t = K_{diff} t^{1/2} + C$	The values of $K_{diff}$ and $C$ were calculated from the slope and intercept of the plot of $q_t$ vs. $t^{1/2}$ , respectively	$K_{diff}$	1.1576
			$C$	0.0818
			$R^2$	0.9718
Elovich	$q_t = 1/\beta \ln(\alpha\beta) + 1/\beta \ln(t)$	Plot the values of $(q_t)$ vs. $\ln(t)$ to give a linear relationship from which $\alpha$ and $\beta$ can be determined from the slope and intercept, respectively	$\beta$	0.0743
			$\alpha$	0.241
			$R^2$	0.9248
			$q_e$ (exp)	95.0304

Table 3  
Thermodynamic parameters for the adsorption of MR onto MWCNT

Parameters	$C_0$ (mg/L)	Temperature, K				
		293	303	313	323	333
MR	$k_c$	18.6	25.6	34.5	45.7	59.6
	$\Delta G^\circ$ (kJ/mol)	-7.1	-8.2	-9.2	-10.3	-11.3
Parameters		MR				
$\Delta S^\circ$ (J/mol K)		105.0				
$\Delta H^\circ$ (kJ/mol)		+23.7				
$E_a$ (kJ/mol)		22.9				
$S^*$		$4.2 \times 10^{-6}$				

the intraparticle diffusion model another model, such as second-order kinetic model, can act to control the adsorption process.

### 3.9. Thermodynamic study

The thermodynamic parameters including Gibbs free energy, enthalpy, and entropy changes were calculated to evaluate the thermodynamic feasibility and the spontaneous nature of the adsorption process. The increase in MR uptake with the increase in temperature indicated the endothermic nature of the adsorption process and the negative values of Gibbs free energy suggested the feasibility of the process and spontaneous nature of the adsorption of MR onto MWCNTs. The thermodynamic constants were obtained from the following equations:

$$\Delta G^\circ = -RT \ln K_o \quad (9)$$

where  $\Delta G^\circ$  is the free energy change ( $\text{kJ mol}^{-1}$ ),  $R$  is the universal gas constant ( $8.314 \text{ J/mol K}$ ),  $K_o$  is the thermodynamic equilibrium constant, and  $T$  is the absolute temperature (K). Increasing the negative value of Gibbs free energy with the increase in temperature showed the high tendency of MWCNT.  $K_o$  values were calculated from the relation  $\ln q_e/C_e$  vs.  $q_e$  at different temperatures and extrapolating to zero [38,39] and the calculated thermodynamic parameters are listed in Table 3. The negative  $\Delta G^\circ$  values confirm the spontaneous nature and feasibility of the adsorption process. The values of other parameters, such as enthalpy ( $\Delta H^\circ$ ) and entropy ( $\Delta S^\circ$ ) changes, were determined from Van't Hoff equation:

$$\ln K^\circ = (\Delta S^\circ/R) - (\Delta H^\circ/RT) \quad (10)$$

The  $\Delta H^\circ$  and  $\Delta S^\circ$  values can be calculated from the slope and intercept of the Van't Hoff plot ( $\ln K^\circ$  vs.  $1/T$ ), respectively. The positive value of  $\Delta H^\circ$  confirmed the endothermic nature of the adsorption process, while the positive  $\Delta S^\circ$  value suggested an increase in the randomness at the solid/solution interface during the adsorption of MR onto MWCNTs. To assertion that the physical adsorption is the predominant mechanism, the values of activation energy ( $E_a$ ) and sticking probability ( $S^*$ ) were estimated from the experimental data using a modified Arrhenius type equation related to surface coverage ( $\theta$ ) as follows [40]:

$$S^* = (1 - \theta)e^{-(E_a/RT)} \quad (11)$$

The sticking probability,  $S^*$ , is a function of the adsorbate/adsorbent system under investigation, its value lies in the range of  $0 < S^* < 1$  and is dependent on the temperature of the system. The parameter  $S^*$  indicates the measure of the potential of an adsorbate to remain on the adsorbent indefinite. The surface coverage ( $\theta$ ) can be calculated from the following equation:

$$\theta = [1 - C_e/C_0] \quad (12)$$

The activation energy and sticking probability were estimated from a plot of  $\ln(1-\theta)$  vs.  $1/T$ . The activation energy,  $E_a$ , calculated from the slope of the plot was found to be  $22.9 \text{ kJ/mol}$  for the adsorption of MR onto MWCNT.

## 4. Conclusion

It was observed that the oxidized MWCNT is an efficient adsorbent for the removal of MR. The influences of experimental parameters, such as initial MR concentration, contact time, initial pH of the aqueous

Table 4

Comparison of performance of proposed method with previously reported (MR) removal

Adsorbent	pH	Concentration (ppm)	Adsorption capacity	Contact time (min)	Ref.
Water-Hyacinth biomass	8	10	$8.85 \times 10^{-2}$ mol/g	180	[41]
Activated carbon	4	25	40.49 mg/g	50	[42]
Banana trunk Fibers	3	500	409 mg/g	120	[43]
Banana Pseudostem fibers	3	500	88.5 mg/g	120	[44]
MWCNT-COOH	4	20	108.7 mg/g	25	This study

solution, amount of MWCNT, and temperature on the MR removal percentage, were investigated. The equilibrium and kinetic studies were investigated for the MR adsorption from aqueous solutions onto MWCNT. The isotherm models, such as Langmuir, Freundlich, Tempkin, and Dubinin–Radushkevich, were evaluated and the equilibrium data were best described by the Langmuir model. The process is endothermic in nature and its kinetics can be successfully fitted to the pseudo-second-order kinetic model with involvement of intraparticle diffusion model. Comparison of characteristics performance of proposed method with some previous MR removal reports (Table 4) shows the priority of the method in terms of lower equilibrium time, higher adsorption capacity, etc.

## References

- [1] A.A. Atia, A.M. Donia, W.A. Al-Amrani, Adsorption/desorption behavior of acid orange 10 on magnetic silica modified with amine groups, *Chem. Eng. J.* 150 (2009) 55–62.
- [2] J.C. Garcia, J.I. Simionato, A.E. Carli da Silva, J. Nozaki, N.E. de Souza, Solar photocatalytic degradation of real textile effluents by associated titanium dioxide and hydrogen peroxide, *Solar Energy* 83 (2009) 316–322.
- [3] M.B. Kasiri, H. Aleboye, A. Aleboye, Degradation of Acid Blue 74 using Fe-ZSM5 zeolite as a heterogeneous photo-Fenton catalyst, *Appl. Catal. B* 84 (2008) 9–15.
- [4] S. Renganathan, W.R. Thilagaraj, L.R. Miranda, P. Gautam, M. Velan, Accumulation of Acid Orange 7, Acid Red 18 and Reactive Black 5 by growing *Schizophyllum commune*, *Biores. Technol.* 97 (2006) 2189–2193.
- [5] R. Sokoohi, V. Vatanpoor, M. Zarrabi, A. Vatani, Adsorption of Acid Red 18 (AR18) by activated carbon from poplar wood—a kinetic and equilibrium study, *E-J. Chem.* 7 (2010) 65–72.
- [6] A. Dabrowski, Adsorption—from theory to practice, *Adv. Colloid Interface.* 93 (2001) 135–224.
- [7] K.K.H. Choy, J.F. Porter, G. McKay, Intraparticle diffusion in single and multicomponent acid dye adsorption from wastewater onto carbon, *Chem. Eng. J.* 103 (2004) 133–145.
- [8] M. Ghaedi, M.N. Biyareh, S. Nasiri Kokhdan, S. Shamsaldini, R. Sahraei, A. Daneshfar, S. Shahriyar, Comparison of the efficiency of palladium and silver nanoparticles loaded on activated carbon and zinc oxide nanorods loaded on activated carbon as new adsorbents for removal of Congo red from aqueous solution: Kinetic and isotherm study, *Mater. Sci. Eng. C* 32 (2012) 725–734.
- [9] H. El Bakouria, J. Useroa, J. Morilloa, A. Ouassini, Adsorptive features of acid-treated olive stones for drin pesticides: Equilibrium, kinetic and thermodynamic modeling studies, *Bioreour. Technol.* 100 (2009) 4147–4155.
- [10] N. Hoda, E. Bayram, E. Ayranci, Kinetic and equilibrium studies on the removal of acid dyes from aqueous solutions by adsorption onto activated carbon cloth, *J. Hazard. Mater.* B137 (2006) 344–351.
- [11] M. Ghaedi, M. Montazerzohori, M.N. Biyareh, K. Mortazavi, M. Soylak, Chemically bonded multiwalled carbon nanotubes as efficient material for solid phase extraction of some metal ions in food samples, *Intern. J. Environ. Anal. Chem.* (in press).
- [12] M. Ghaedi, A. Hassanzadeh, S. Nasiri Kokhdan, Multiwalled carbon nanotubes as adsorbents for the kinetic and equilibrium study of the removal of Alizarin Red S and Morin, *J. Chem. Eng.* 56 (2011) 2511–2520.
- [13] A. Duran, M. Tuzen, M. Soylak, Preconcentration of some trace elements via using multiwalled carbon nanotubes as solid phase extraction adsorbent, *J. Hazard. Mater.* 169 (2009) 466–471.
- [14] M. Tuzen, K.O. Saygi, C. Usta, M. Soylak, *Pseudomonas aeruginosa* immobilized multiwalled carbon nanotubes as biosorbent for heavy metal ions, *Bioresour. Technol.* 99 (2008) 1563–1570.
- [15] M. Tuzen, K.O. Saygi, M. Soylak, Solid phase extraction of heavy metal ions in environmental samples on multiwalled carbon nanotubes, *J. Hazard. Mater.* 152 (2008) 632–639.
- [16] M. Tuzen, M. Soylak, Multiwalled carbon nanotubes for speciation of chromium in environmental samples, *J. Hazard. Mater.* 147 (2007) 219–225.
- [17] M. Ghaedi, A. Shokrollahi, H. Hossainian, S. Nasiri Kokhdan, Comparison of activated carbon and multiwalled carbon nanotube for efficient removal of Eriochrome Cyanine R: Kinetic, isotherm and thermodynamic study of removal process, *J. Chem. Eng. Data* 56 (2011) 3227–3235.
- [18] M. Ghaedi, H. Tavallali, M. Sharifi, S. Nasiri Kokhdan, A. Asghari, Preparation of low cost activated carbon from *Myrtus communis* and pomegranate and their efficient application for removal of Congo red from aqueous solution, *Spectrochim. Acta Part A: Mol. Biomol. Spectrosc.* 86 (2012) 107–114.
- [19] F. Marahel, M. Ghaedi, S. Nasiri Kokhdan, Silver nanoparticle loaded on activated carbon as an adsorbent for the removal of Sudan Red 7B from aqueous solution, *Fresen. Environ. Bull.* 21 (2012) 163–170.
- [20] Y.-S. Ho, Review of second-order models for adsorption systems, *J. Hazard. Mater.* B136 (2006) 681–689.
- [21] B. Fugetsu, S. Satoh, T. Shiba, T. Mizutani, Y. Lin, N. Terui, Y. Nodasaka, K. Sasa, K. Shimizu, T. Akasaka, Caged multiwalled carbon nanotubes as the adsorbents for affinity-based elimination of ionic dyes, *Environ. Sci. Technol.* 38 (2004) 6890–6896.
- [22] M. Ghaedi, J. Tashkhourian, A. Amiri Pebdani, B. Sadeghian, F. Nami Ana, Equilibrium, kinetic and thermodynamic study of removal of reactive orange 12 on platinum nanoparticle loaded on activated carbon as novel adsorbent, *Korean J. Chem. Eng.* 28 (2011) 2255–2261.
- [23] I. Langmuir, The adsorption of gases on plane surfaces of glass, mica and platinum, *J. Am. Chem. Soc.* 40 (1918) 1361–1403.

- [24] M. Ghaedi, S. Zamani Amirabad, F. Marahel, S. Nasiri Kokhdan, R. Sahraei, A. Daneshfar, Synthesis and characterization of Cadmium selenide nanoparticles loaded on activated carbon and its efficient application for removal of Muroxide from aqueous solution, *Spectrochim. Acta, Part A* 83 (2011) 46–51.
- [25] I. Langmuir, The constitution and fundamental properties of solids and liquids, *J. Am. Chem. Soc.* 38 (1916) 2221–2295.
- [26] O. Abdelwahab, Evaluation of the use of loofa activated carbons as potential adsorbents for aqueous solutions containing dye, *Desalination* 222 (2008) 357–367.
- [27] C. Ng, J.N. Losso, W.E. Marshall, R.M. Rao, Freundlich adsorption isotherms of agricultural by-product-based powdered activated carbons in a geosmin–water system, *Biore-sour. Technol.* 85 (2002) 131–135.
- [28] L. Aia, C. Zhang, Z. Chen, Removal of methylene blue from aqueous solution by a solvothermal-synthesized graphene/magnetite composite, *J. Hazard. Mater.* 192 (2011) 1515–1524.
- [29] M. Ghaedi, H. Khajesharifi, A.H. Yackuri, M. Roosta, R. Sahraei, A. Daneshfar, Cadmium hydroxide nanowire loaded on activated carbon as efficient adsorbent for removal of Bromocresol Green, *Spectrochim. Acta, Part A* 86 (2012) 62–68.
- [30] S. Lagergren, *Kungliga Svenska Vetenskapsakademiens, Handlingar* 24 (1898) 1–39.
- [31] M.J. Iqbal, M.N. Ashiq, Adsorption of dyes from aqueous solutions on activated charcoal, *J. Hazard. Mater.* B139 (2007) 57–66.
- [32] Y.S. Ho, G. McKay, D.A.J. Wase, C.F. Foster, *Adsorpt. Sci. Technol.* 18 (2000) 639–650.
- [33] D.M. Ruthven, K.F. Loughlin, The effect of crystallite shape and size distribution on diffusion measurements in molecular sieves, *Chem. Eng. Sci.* 26 (1971) 577–584.
- [34] M. Ghaedi, Sh. Heidarpour, S. Nasiri Kokhdan, R. Sahraie, A. Daneshfar, B. Brazesh, Comparison of silver and palladium nanoparticles loaded on activated carbon for efficient removal of methylene blue: Kinetic and isotherm study of removal process, *Powder Technol.* 228 (2012) 18–25.
- [35] M. Ghaedi, A. Hekmati, S. Khodadoust, R. Sahraei, A. Daneshfar, A. Mihandoost, M.K. Purkait, Cadmium telluride nanoparticles loaded on activated carbon as adsorbent for removal of sunset yellow, *Spectrochim. Acta, Part A* 90 (2012) 22–27.
- [36] D. Ozdes, C. Duran, H.B. Senturk, Adsorptive removal of Cd (II) and Pb(II) ions from aqueous solutions by using Turkish illitic clay original research article, *J. Environ. Manage.* 92 (2011) 3082–3090.
- [37] M.S. Chiou, H.Y. Li, Equilibrium and kinetic modeling of adsorption of reactive dye on cross-linked chitosan beads, *J. Hazard. Mater. B* 93 (2002) 233–248.
- [38] I.D. Mall, V.C. Srivastava, N.K. Agarwal, I.M. Mishra, Adsorptive removal of malachite green dye from aqueous solution by bagasse fly ash and activated carbon-kinetic study and equilibrium isotherm analyses, *Colloids Surf. A* 264 (2005) 17–28.
- [39] K. Kannan, M.M. Sundaram, Kinetics and mechanism of removal of methylene blue by adsorption on various carbons—a comparative study, *Dyes Pigm.* 51 (2001) 25–40.
- [40] A. Aziz, M.S. Ouali, E.H. Elandaloussi, L.C.D. Menorval, M. Lindheimer, Chemically modified olive stone: A low-cost sorbent for heavy metals and basic dyes removal from aqueous solutions, *J. Hazard. Mater.* 163 (2009) 441–447.
- [41] T. Tarawou, M. Horsfall Jr, J.L. Vicente, Adsorption of methyl red by water-hyacinth (*eichornia crassipes*) biomass, *Chem. Biodivers.* 4 (2007) 2236–2246.
- [42] T. Santhi, S. Manonmani, T. Smitha, Removal of methyl red from aqueous solution by activated carbon prepared from the *Annona squamosa* seed by adsorption, *Chem. Eng. Res. Bull.* 14 (2010) 11–18.
- [43] Mas Rosemal, H. Mas Haris, Kathiresan Sathasivam, Scholars research library, *Arch. Appl. Sci. Res.* 2(5) (2010), 209–216.
- [44] M. Rosemal, H. Mas Haris, K. Sathasivam, The removal of methyl red from aqueous solutions using banana pseudostem fibers, *Am. J. Appl. Sci.* 6(9) (2009) 1690–1700.